Theoretical study of forbidden unique and non-unique beta decays of medium-heavy nuclei

Nael Soukouti

A Thesis Presented For The Degree of
Master's In Theoretical Nuclear Physics

UNIVERSITY OF JYVÄSKYLÄ

Department Of Physics
Finland
Supervisor: Jouni Suhonen
February 2015

Contents

List of Tables

List of Figures

Abstract

This Master's Thesis concerns using the quasi-particle random phase approximation model in the study of β decay. The study is done for the transition from the 2_1^- state of odd-odd nuclei to the isobaric neighbour's (even-even nuclei) ground state and some low-lying excited states. The mass numbers of the studied nuclei are A=72, 74, 76, 78, 82, 84, 86, 88, 92, 94, 122, 124, 126, 132. The computed comparative β decay half-lives log(ft) values are compared with the experimental results.

Introduction

The beta decay theory is a good test bench for nuclear models. It is accurate in describing the most typical beta transitions and the kinematic part of the theory is fully universal. The realization that neutrinos are massive, increased the interest in investigating their intrinsic properties and motivate the scientific community to do more efforts to understand the neutrino mass generation mechanism. The absolute neutrino mass scale and the neutrino mass spectrum became the main goal of neutrino experiments. Part of this work have been used to assist these efforts.

The starting point to calculate the comparative β decay half-life log(ft) value in this work is choose an even-even nucleus that is used as reference nucleus. To make the calculation lighter, the configuration space of the reference nucleus is divided into two parts [1]. The innermost nuclear orbitals form an inert nuclear core and only the outer orbitals contribute to the interactions that lead to the formation of excited states of the nucleus. These active outer nuclear orbitals of the reference is called the valance space.

The ground state of the reference nucleus can be obtained from BCS theory [1, 2]. The excited states of those reference nuclei can then be described as proton-proton (neutron-neutron) quasi-particles pairs on the top of the ground state (Charge conserving QRPA). While the ground state and excited states of neighbouring odd-odd nuclei can then be described as proton-neutron quasi-particles pairs on the top of the ground state of the reference nucleus (Charge changing pnQRPA).

This Thesis is organized as follows: The first section of this text concentrates on the theoretical description of nuclear states. The second section provides a brief theory of Unique and Non-Unique first-forbidden beta decay. In the third section of the text the theoretical framework is applied to the β decay for selected sets of nuclei. The final section contains the conclusions.

1 Theoretical Description of Nuclear States

In this section the particle nuclear mean field is introduced first. Then the quasi-particle description is elucidated by briefly summarizing the BCS, QRPA and the pnQRPA.

1.1 Nuclear Mean Field

The mean field's concept is broadly used for the description of interacting many-body systems where the A-nucleon Schrödinger equation can not be

solved exactly, at least for $A > 10$. Therefore one has to look for reasonable approximate methods to solve this many-body problem of strongly interacting system of particles. This could be done in a straightforward way by converting the strongly interacting system of particles into a system of weakly interacting *quasi-particles*. In the first approximation the system of quasi-particles can be treated as a set of non-interacting quasi-particles. The standard way to do that is to use the so-called mean field approximation. The significant idea behind this approximation is to treat the many-body system and describe the interaction of one particle with the remaining particles in system by an average potential created by the other ones. Not by summing up all mutual two-body interactions of the particles. In addition one should be cognizant that the remaining interactions commonly named residual interactions, can usually be treated by perturbation theory. The possible form of the nuclear Hamiltonian is

$$H = [T + V_{\rm MF}] + [V - V_{\rm MF}] = H_{\rm MF} + V_{\rm RES}, \tag{1}$$

where

$$H_{\rm MF} = T + V_{\rm MF} = \sum_{i=1}^{A} [t(r_i) + v(r_i)] = \sum_{i=1}^{A} h(r_i), \tag{2}$$

$V_{\rm RES}$ is the residual interaction (In the mean field approach any interaction that is not accounted for is considered as residual interaction), and $h(r_i)$ is the one-body Hamiltonian.

In the mean-field approximation each nucleon can be viewed as moving in an external field created by the remaining $A - 1$ nucleons. This external potential $V_{\rm MF}$ in Eq. (1) is commonly and simply represented by central potential known by the name *Woods-Saxon* potential [1]. This potential has been used widely, has enjoyed success and its form can be seen below:

$$v_{\rm ws} = \frac{V_0}{1 + e^{(r-R)/a}}, \tag{3}$$

where in its usual parametrization the nuclear radius R and the surface diffuseness a are taken to be [1]

$$R = r_0 A^{1/3} = 1.27 A^{1/3} fm\,;\; a = 0.67 fm. \tag{4}$$

The depth V_0 of the potential is chosen according to the relation

$$V_0 = (51 \pm 33 \frac{N - Z}{A}). \tag{5}$$

The central potential alone does not reproduce the experimentally observed qualitative behaviour of single-particle energies in the mean field. To

achieve this we need to add an additional term resulting from the spin- orbit interaction, which we denoted in Eq. (1) as $V_{\rm RES}$.

Including the Woods-Saxon potential $\upsilon_{\rm WS}$ the one-body Hamiltonian is [1]

$$\begin{aligned} h(r)|nl\frac{1}{2}jm\rangle &= \left[-\frac{\hbar}{2m_N}(\nabla_r^2 - \frac{\mathbf{L}^2/\hbar^2}{r^2}) + \upsilon_{WS}(r) + \upsilon_c(r) + \upsilon_{\rm LS}(r)\mathbf{L}\cdot\mathbf{S}\right]|nl\frac{1}{2}jm\rangle, \\ &= \varepsilon_{nlj}|nl\frac{1}{2}jm\rangle, \end{aligned} \tag{6}$$

the symbol ∇_r^2 denotes the usual radial derivative, $\upsilon_c(r)$ is Coulomb potential and it applies to protons only and $\upsilon_{\rm LS}(r)$ is the spin-orbit term

$$\upsilon_{\rm LS}(r) = \upsilon_{\rm LS}^{(0)}(\frac{r_0}{\hbar})^2\frac{1}{r}\left[\frac{d}{dr}\frac{1}{1+e^{(r-R)/a}}\right], \tag{7}$$

$$\upsilon_{LS}^{(0)} = 0.44V_0. \tag{8}$$

The latter part $V_{\rm RES}$ in Eq. (1), the residual interaction, containing all the two-body interaction, is effectively suppressed by maximizing the first part $\rm H_{MF}$, and it can then be treated as small perturbation. This procedure effectively replaces the A strongly interacting nucleons with weakly interacting mean-field quasi-particles and this is called nuclear mean-field approximation.

1.2 BCS Model

In the BCS theory the basic constituents of nuclei are not particle or holes but rather quasi-particles that have both particle and hole component. In other words they are in fact generalized fermions which they are simultaneously partly particles and partly holes with certain amplitudes. Since these hybrid particles or what we called before quasi-particles, are moving in an additional field - the pairing field - generated by the short-range forces. One can easily recognize the importance of the pairing phenomena in nuclei and it makes the BCS theory essential in describing the nuclear structure. The starting point in this formalism is the ansatz for the BCS ground state [1]

$$|\text{BCS}\rangle = \prod_{\alpha>0}(u_a - \upsilon_a c_\alpha^\dagger \tilde{c}_\alpha^\dagger)|\text{HF}\rangle. \tag{9}$$

The notation here is $\alpha = (a, m_\alpha)$ and $a = (n_a, l_a, j_a)$ for the quantum number of a single-particle orbital, u_a and v_a are the occupation amplitudes. The

creation and annihilation operators $a^\dagger_\alpha$ and a_α are defined via the Bogoliubov-Valatin transformation [1]

$$a^\dagger_\alpha = u_a c^\dagger_\alpha + \upsilon_a \tilde{c}_\alpha, \tag{10}$$

$$\tilde{a}_\alpha = u_a \tilde{c}_\alpha - \upsilon_a c^\dagger_\alpha. \tag{11}$$

The standard nuclear Hamiltonian in quasi-particle representation is

$$H = H_0 + \sum_b \hat{j}_b E_b [a^\dagger_b \tilde{a}_b]_{00} + V_{\mathrm{RES}}. \tag{12}$$

In this Hamiltonian the first two terms carry most of the nucleon-nucleon short-range interaction. The information in this model is condensed in the BCS equations below which arise from a variational procedure :

$$\begin{aligned}
u_a &= \frac{1}{\sqrt{2}}\sqrt{1+\frac{\eta_a}{E_a}}\,(\text{occupation amplitudes}),\\
\upsilon_a &= \frac{1}{\sqrt{2}}\sqrt{1-\frac{\eta_a}{E_a}}\,(\text{occupation amplitudes}),\\
E_a &= \sqrt{\eta_a^2+\Delta_a^2}\,(\text{quasiparticle energy}),\\
2\hat{j}_a\Delta_a &= -\sum_b \frac{\hat{j}_b\Delta_b}{\sqrt{\eta_b^2+\Delta_b^2}}\langle aa;0|V|bb;0\rangle\,(\text{gap equation}),\\
\bar{n} &= \sum_a \hat{j_a}^{\,2}\upsilon_a^2 = \frac{1}{2}\sum_a \hat{j_a}^{\,2}(1-\frac{\eta_a}{E_a})\,(\text{average particle number}).
\end{aligned} \tag{13}$$

Where η_a and Δ_a are abbreviations for certain blocks of terms, are called the effective single-particle energy and paring gap respectively [1]. In practice the parameters of the BCS calculation are adjusted to reproduce the experimental paring gaps. Here in this thesis the empirical paring gaps have been computed from the three-point formula [1]

$$\Delta_p = \frac{1}{4}(-1)^{Z+1}(S_p(A+1,Z+1) - 2S_p(A,Z) + S_p(A-1,Z-1)), \tag{14}$$

$$\Delta_n = \frac{1}{4}(-1)^{N+1}(S_n(A+1,Z) - 2S_n(A,Z) + S_n(A-1,Z)), \tag{15}$$

by using the proton (S_p) and neutron (S_n) separation energies [3], where Z and N are the numbers of protons and neutrons respectively of the even-even reference nucleus.

1.3 QRPA & pnQRPA

The quasiparticle random-phase approximation (QRPA) is adopted to construct the excited states of the even-even nuclei. And the proton-neutron quasiparticle random-phase approximation (pnQRPA) is also adopted to construct the excited states of the odd-odd nuclei. The first step in both the QRPA and pnQRPA formalism is to solve the BSC equation. After that we start the construction for the nuclear states by forming all two-quasiparticle states with good angular momentum J_ω and parity π_ω. The state vector for excitation $\omega = (J_\omega, \pi_\omega, k_\omega)$ is then given by [1]

$$|\omega\rangle = Q^\dagger_\omega |(\text{pn})\text{QRPA}\rangle, \tag{16}$$

here $|(\text{pn})\text{QRPA}\rangle$ denotes the vacuum state of either the QRPA or pnQRPA. The excitation operator $Q^\dagger_\omega$ is defined in QRPA as [1]

$$Q^\dagger_\omega = \sum_{a\leq b} \left[X^\omega_{ab} N_{ab}(J_\omega)[a^\dagger_a a^\dagger_b]_{J_\omega M_\omega} + Y^\omega_{ab} N_{ab}(J_\omega)[\tilde{a}_a \tilde{a}_b]_{J_\omega M_\omega} \right], \tag{17}$$

where the indices a, b run over all two-proton and two-neutron configuration within the chosen valance space, so that non of them is counted twice. The quantity N_{ab} is a normalization constant [1].

In a similar fashion the pnQRPA creation operator $Q^\dagger_\omega$ is given by[1]

$$Q^\dagger_\omega = \sum_{pn} \left[X^\omega_{pn}[a^\dagger_p a^\dagger_n]_{J_\omega M_\omega} + Y^\omega_{pn}[\tilde{a}_p \tilde{a}_n]_{J_\omega M_\omega} \right], \tag{18}$$

where the sum runs over all possible proton-neutron configurations in the adopted valence space. In both the QRPA and pnQRPA the amplitudes X^ω and Y^ω can be found from the matrix equation [1]

$$\begin{pmatrix} A & B \\ -B^* & -A^* \end{pmatrix} \begin{pmatrix} X^\omega \\ Y^\omega \end{pmatrix} = E_\omega \begin{pmatrix} X^\omega \\ Y^\omega \end{pmatrix} \tag{19}$$

where E_ω is the excitation energy of the state $|\omega\rangle$. Here A is a hermitian matrix known as the quasiparticle Tamm-Dancoff (QTDA) matrix in the QRPA and the pnQTDA matrix in the pnQRPA. B is a symmetric matrix which accounts for the ground-state correlations (correlation matrix).

2 First-Forbidden Beta Decay

In this section we briefly introduce the theory of first-forbidden beta decay. In first-forbidden beta decay modes leptons are emitted in p-wave and there are

also contributions coming from the small components of the relativistic Dirac wave function. There are four types of nuclear matrix element that emerge from p-wave leptons, and there are two types of nuclear matrix element that emerge from the small components of Dirac spinors. All these six matrix elements contribute to the first-forbidden nuclear beta decay. Each of the operators changes the parity. This means that the initial and final nuclear states must have opposite parities, i.e. $\pi_i \pi_f = -1$.

2.1 First-Forbidden Unique Beta Decay

An appropriate simplification can be achieved when $\Delta J = 2$. Then there is only the tensor-axial matrix element from six matrix elements (the one with the largest total angular momentum content) which contributes. The shape function of a first-forbidden unique $\beta^{\pm}$ transition which contains the tensor-axial nuclear matrix element and the appropriate lepton kinematics can be taken [4]

$$S_{1u}^{(\mp)}(Z_f, \varepsilon) = F_{1u}(\pm Z_f, \varepsilon) p\varepsilon (E_0 - \varepsilon)^2 \tag{20}$$

$$= [F_0(\pm Z_f, \varepsilon)(E_0 - \varepsilon)^2 + F_1(\pm Z_f, \varepsilon)(\varepsilon^2 - 1)] p\varepsilon (E_0 - \varepsilon)^2,$$

where the functions $F_0(\pm Z_f, \varepsilon)$ and $F_1(\pm Z_f, \varepsilon)$ are Fermi functions taking into account the coulomb interaction between the final-state lepton and the residual nucleus. The endpoint energy E_0 is given by

$$E_0 = \frac{Q_{\beta-} + m_e c^2}{m_e c^2} \ (\text{for } \beta^- \text{ decay}), \tag{21}$$

and

$$E_0 = \frac{Q_{\beta+} + m_e c^2}{m_e c^2} = \frac{Q_{\text{EC}} - m_e c^2}{m_e c^2} \ (\text{for } \beta^+ \text{ decay}). \tag{22}$$

Where the Q values ($Q_{\beta+}$, $Q_{\beta-}$ and Q_{EC}) of nuclear beta decays were defined in [1] as the total kinetic energies of the final-state leptons. The phase space factor is now

$$f_{1u}^{(\mp)} = \int_1^{E_0} S_{1u}^{(\mp)}(Z_f, \varepsilon) d\varepsilon. \tag{23}$$

The ft value for the first-forbidden unique beta decay can be defined as

$$ft \equiv f_{1u} t_{1/2} = \frac{\kappa}{\frac{1}{12} B_{1u}} \ ; B_{1u} = \frac{g_A^2}{2J_i + 1} |M_{1u}|^2, \tag{24}$$

with κ given by

$$\kappa \equiv \frac{2\pi^3 h^7 \ln 2}{m_e^5 (2\pi)^7 c^4 G_F^2} = 6147s, \tag{25}$$

and

$$f_{1u} \equiv f_{1u}^{(-)} \,(\text{for}\, \beta^- \,\text{decay});\;\; \mathrm{f_{1u}} \equiv \mathrm{f_{1u}^{(+)}} + \mathrm{f_{1u}^{(EC)}} \;(\text{for}\, \beta^+/\text{EC}\, \text{decay}). \tag{26}$$

The ft value in Eq. (24) is a phase-space independent and depends only on nuclear structure.

2.2 First-Forbidden Non-Unique Beta Decays

In the first-forbidden non-unique beta decay all the six decay operators are available to produce a given transition. The shape functions of a first-forbidden non-unique $\beta^{\pm}$ transition which contains these six nuclear matrix element with the appropriate phase-space factors of the lepton kinematics have a complicated formula. In compact fashion they are denoted as the following:

$$S_{K=1} = \begin{cases} S_{K=1}^{(-)}, & \text{for } \beta^- \text{ decay} \\ S_{K=1}^{(+)} + S_{K=1}^{(EC)}, & \text{for } \beta^+ \text{ / EC decay.} \end{cases} \tag{27}$$

The convenient definition for ft value can be as follow [5]

$$ft \equiv f_0^{(-)} t_{1/2} = \frac{\kappa}{S_{K=1}}, \tag{28}$$

where the $f_0^{(-)}$ is scaling quantity to normalize the integrated phase-space factors present in Eq. (27).

3 Results and Discussion

In this section the theoretical framework is put into a test. Here we have performed calculations of $\log(ft)$ for the sets of nuclei listed in Table1 (*The sets of nuclei in the Table 1 are classified according to valance space of the single particle orbitals for the reference nuclei*). The listed nuclei decay by β channels from the 2_1^- state of odd-odd nucleus, to the two groups of states of the reference nucleus. First group consists of the 0^+ ground state, 0_2^+ and 4_1^+ excited states where the corresponding decays are first-forbidden unique beta decays. Second group includes the $2_1^+$and 2_2^+ states where the corresponding decays are first-forbidden non-unique beta decay. We have

done QRPA and pnQRPA calculations to build up the appropriate nuclear structures for participant initial and final states. We compare our results with the experimental results to see how well the chosen pnQRPA framework works.

Table 1: The nuclei discussed in the present work classified according to their decay channels. The reference nuclei are denoted in parentheses.

Set's name	Decaying via β^-	Decaying via β^+
Set1		^{72}As(Ge)
	^{74}As(Se)	^{74}As(Ge)
	^{76}As(Se)	^{76}As(Ge)
	^{78}As(Se)	
	^{82}Br(Kr)	
	^{84}Br(Kr)	
	^{84}Rb(Sr)	^{84}Rb(Kr)
	^{86}Rb(Sr)	^{86}Rb(Kr)
	^{88}Rb(Sr)	
	^{92}Y(Zr)	
	^{94}Y(Zr)	
Set2	^{122}Sb(Te)	^{122}Sb(Sn)
		^{124}I(Te)
	^{126}I(Xe)	^{126}I(Te)
		^{132}La(Ba)

3.1 Single-Particle States

The single-particle energies were computed by using the Woods-Saxson potential. The adopted valance space for the reference nuclei in the set 1 (see Table1) consists of proton single-particle orbitals 0f, 1p, 0g, 1d, 2s and $0h_{11/2}$ and the neutron single-particle orbitals are the same as the proton ones. The adopted valance space for the nuclei in the set 2 (Table1) consists of the proton single-particle orbitals 0f, 1p, 0g, 1d, 2s, 0h, 1f and 2p and the neutron single-particle orbitals are the same as the proton ones. The obtained single-particle energies for protons and neutrons as functions of the atomic number "A" are plotted in Figs 1-10. The energies vary gradually and that is consistent with the smooth evolution of the Woods-Saxon energies with the presently used parametrization. We should mention that in the set 1 we corrected the energies of the level $1d_{5/2}$ for the references elements ^{76}Ge, ^{84}Kr, ^{86}Kr, ^{86}Sr manually relative to the $2s_{1/2}$ level to produce a smooth trend of

energies. And also we did the same in set 2 for the reference element ^{122}Sn by changing the $0h_{9/2}$ orbit manually relative to the $1d_{3/2}$ orbit.

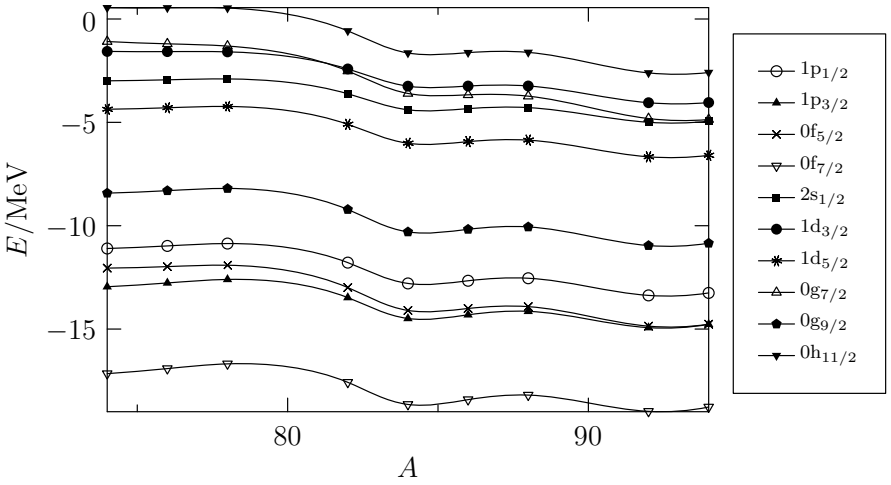

Figure 1: Neutron energy levels for the 1st set of nuclei excluding ^{84}Kr (same mass number as ^{84}Sr) decaying via β^-.

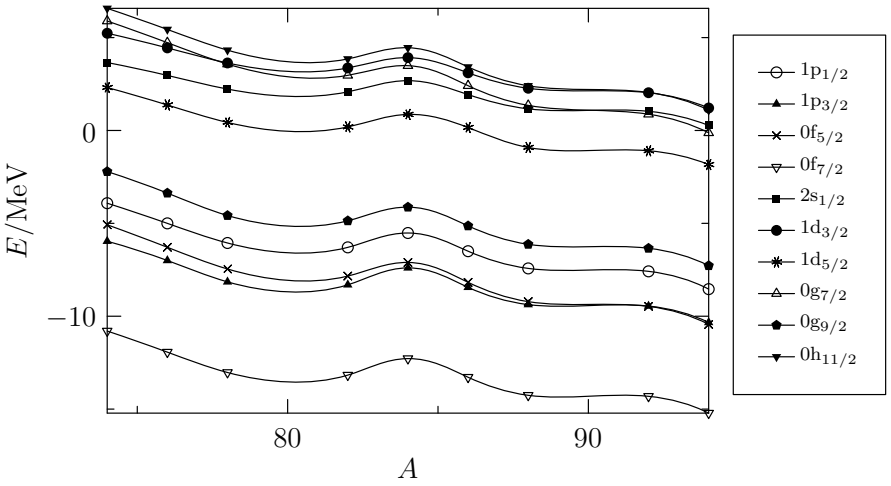

Figure 2: Proton energy levels for the 1st set of nuclei excluding ^{84}Kr (same mass number as ^{84}Sr) decaying via β^-.

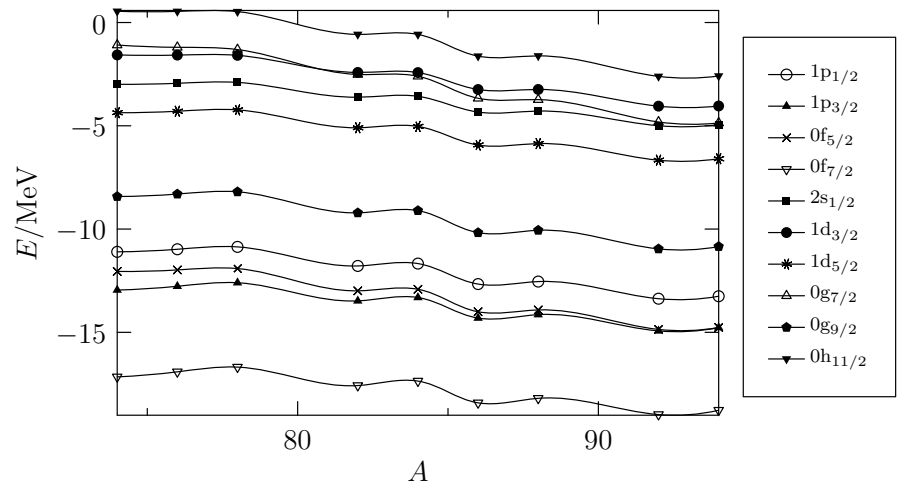

Figure 3: Neutron energy levels for the 1st set of nuclei excluding ^{84}Sr (same mass number for ^{84}Kr) decaying via β^-.

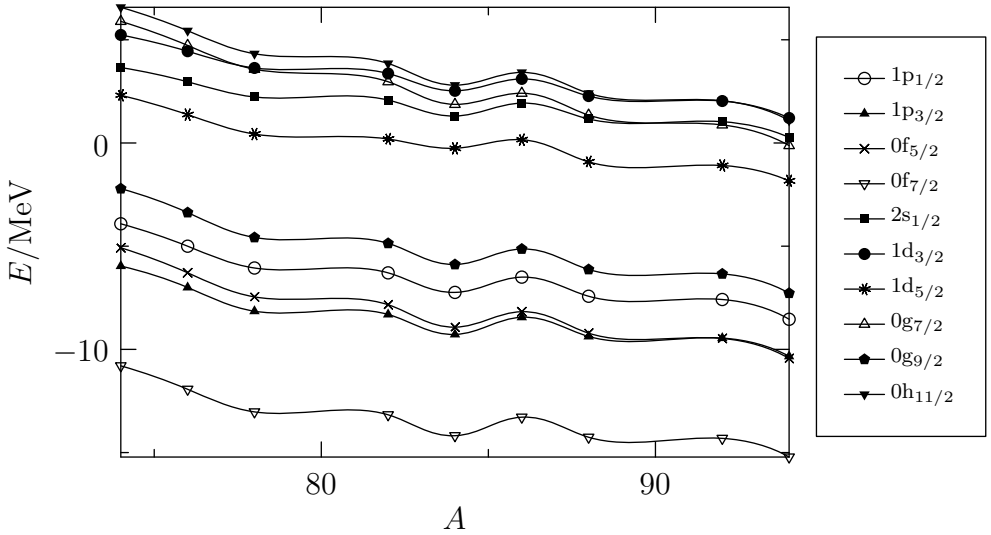

Figure 4: Proton energy levels for the 1st and set of nuclei excluding ^{84}Sr (same mass number as ^{84}Kr) decaying via β^-.

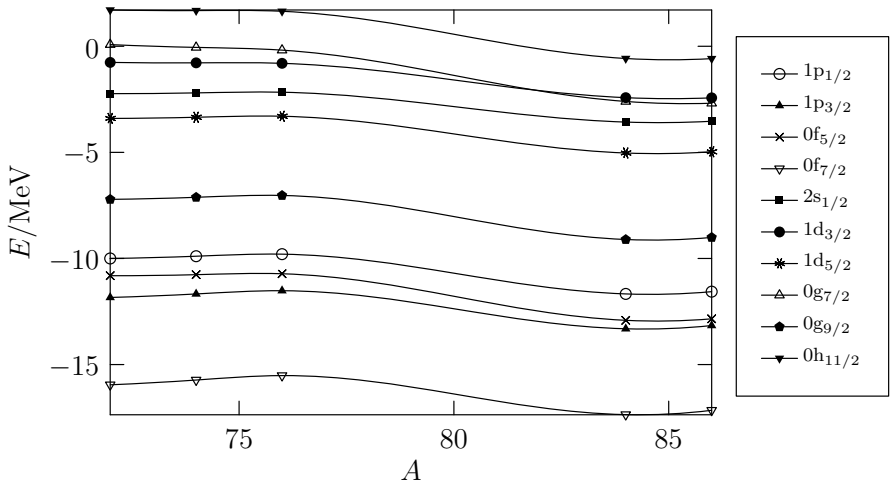

Figure 5: Neutron energy levels for the 1st set of nuclei decaying via β^+.

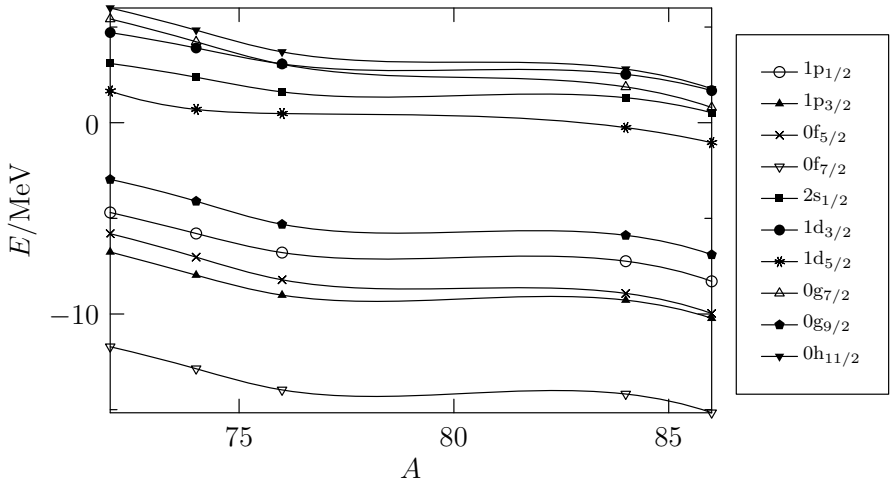

Figure 6: Proton energy levels for the 1st set of nuclei decaying via β^+.

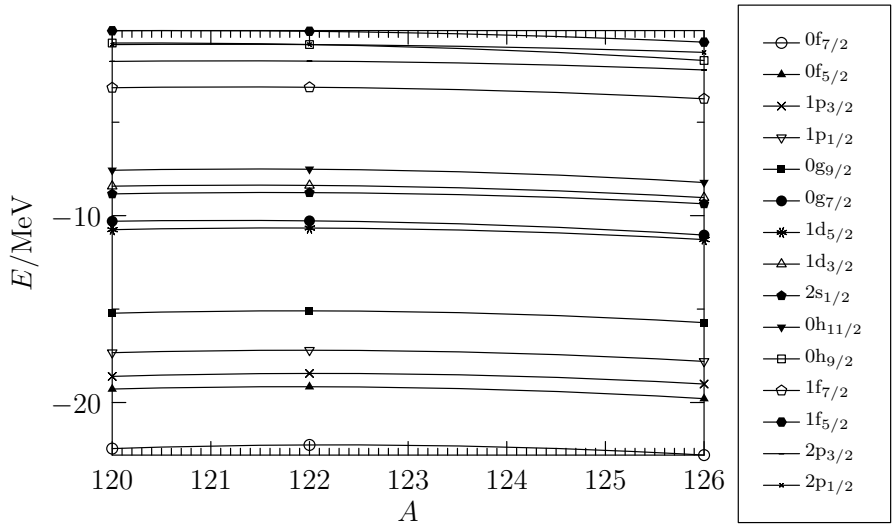

Figure 7: Neutron energy levels for the 2nd set of nuclei decaying via β^- in addition to ^{120}Te nucleus.

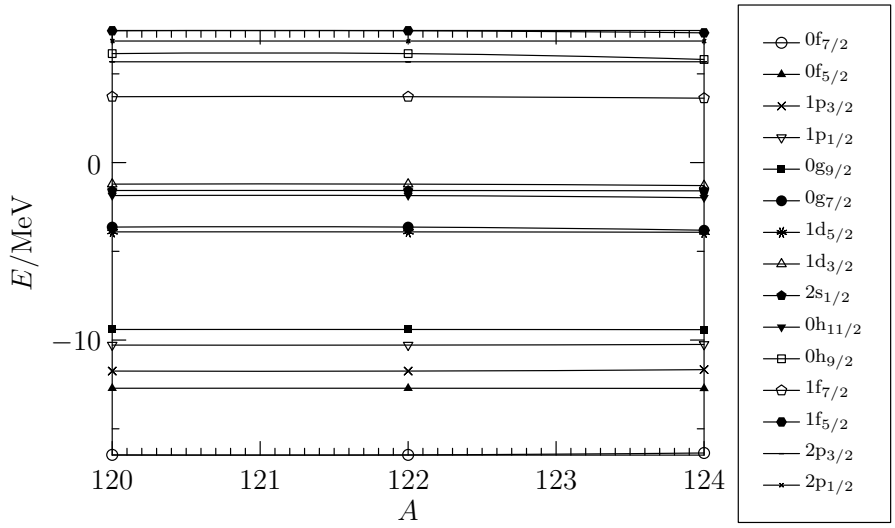

Figure 8: Proton energy levels for the 2nd set of nuclei decaying via β^- in addition to ^{120}Te nucleus.

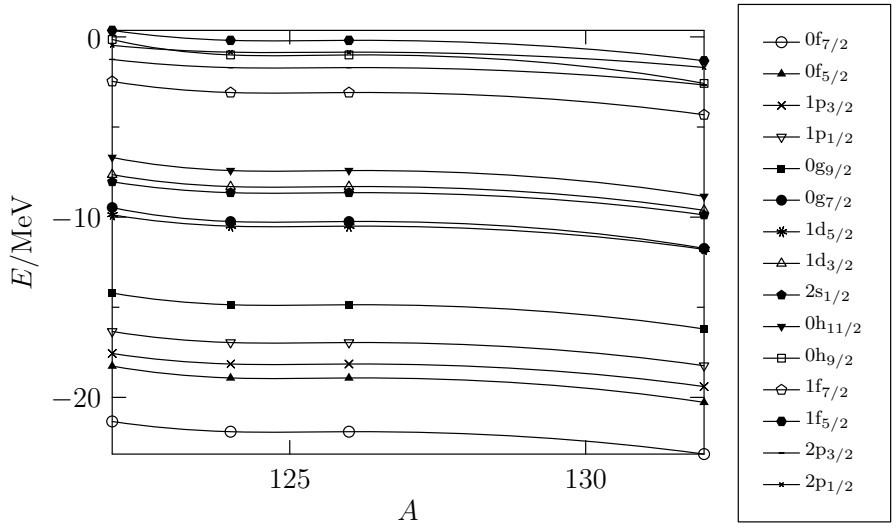

Figure 9: Neutron energy levels for the 2nd set of nuclei decaying via β^+.

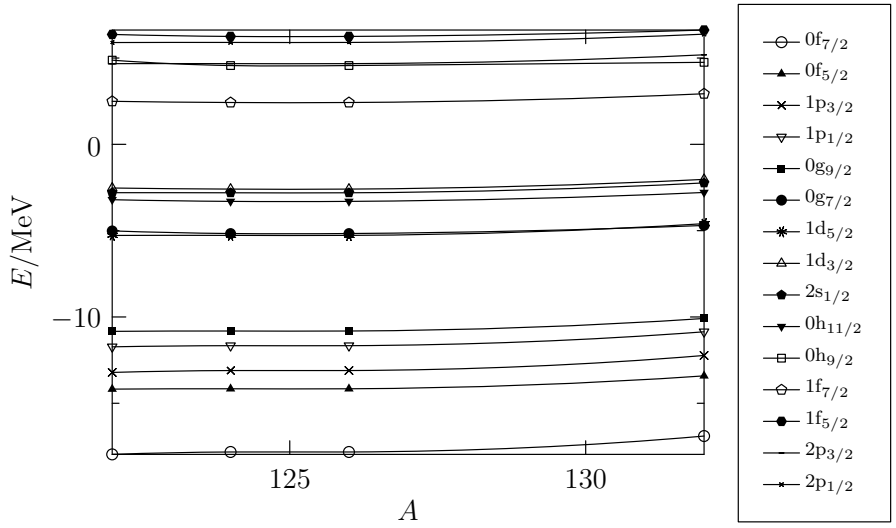

Figure 10: Neutron energy levels for the 2nd set of nuclei decaying via β^+.

3.2 BCS Calculation

In this step the quasi-particles were defined by performing BCS calculations for protons and neutrons. We considered the $Z_{\text{core}} = 20$ and $N_{\text{core}} = 20$ for all nuclei. The interaction was scaled by a constant $g_{\text{p}}^{\text{pair}}$ for protons and $g_{\text{n}}^{\text{pair}}$ for neutrons, so that the energy of the lowest quasi-particle state was roughly equal to the empirical pairing gap Δ_{p} and Δ_{n} computed from the three-point formulas (14) and (15), by using separation energy for the proton (S_p) and for neutron (S_n) obtained from [3]. Table 2 show the adjusted values $g_{\text{p}}^{\text{pair}}$, $g_{\text{n}}^{\text{pair}}$ to reproduce the empirical pairing gaps Δ_{p} and Δ_{n}.

Table 2: The adopted values $g_{\text{n}}^{\text{pair}}$ and $g_{\text{p}}^{\text{pair}}$ to make the energy of the lowest quasi-particle state roughly equal to the empirical paring gaps Δ_{n} & Δ_{p}.

Nucles	Δ_{n}	$g_{\text{n}}^{\text{pair}}$	Δ_{p}	$g_{\text{p}}^{\text{pair}}$
^{72}Ge	1.826	1.0845	1.488	1.0215
^{74}Ge	1.776	1.2385	1.570	1.0635
^{74}Se	1.813	1.1506	1.815	1.1214
^{76}Ge	1.570	1.2006	1.521	1.0390
^{76}Se	1.715	1.2212	1.710	1.0913
^{78}Se	1.653	1.2464	1.618	1.0575
^{82}Kr	1.647	1.2575	1.633	0.7900
^{84}Kr	1.614	1.2295	1.432	0.9487
^{84}Sr	1.616	1.2482	1.871	1.1000
^{86}Kr	1.771	1.2390	1.355	0.9108
^{86}Sr	1.507	1.1970	1.622	1.0265
^{88}Sr	1.86	0.9640	1.382	0.9635
^{92}Zr	0.72	0.9640	1.265	0.9389
^{94}Zr	0.811	0.9530	1.303	0.9491
^{122}Sn	1.379	1.071	1.76	0.9865
^{122}Te	1.376	1.017	1.326	1.037
^{124}Te	1.338	1.052	1.251	0.9865
^{126}Te	1.343	1.0934	1.169	0.9525
^{126}Xe	1.3	1.0394	1.302	0.998
^{132}Ba	1.24	1.0705	1.377	1.0014

3.3 QRPA Calculation

In this step we constructed the exited states 2_1^+, 2_2^+, 0_2^+ and 4_1^+ for even-even nucleus by using the QRPA. In the QRPA matrix the particle-hole part as scaled by a parameter called g_{ph}. We adjusted g_{ph} to get roughly the experimental energy value for the 2_1^+ state. The adopted values are presented in Table 3.

Table 3: The g_{ph} values for the even-even refrence nuclei.

	$E(2_1^+)$ (MeV)		
Nucles	Experimental	Theoretical	g_{ph}
^{72}Ge	0.834	0.835	0.954
^{74}Ge	0.596	0.596	0.869
^{74}Se	0.644	0.634	0.921
^{76}Ge	0.563	0.593	0.801
^{76}Se	0.560	0.559	0.837
^{78}Se	0.614	0.613	0.833
^{82}Kr	0.777	0.777	0.799
^{84}Kr	0.882	0.882	0.886
^{84}Sr	0.793	0.794	0.916
^{86}Kr	1.565	1.565	1.202
^{86}Sr	1.077	1.108	1.008
^{88}Sr	1.836	1.837	0.780
^{92}Zr	0.935	0.934	0.660
^{94}Zr	0.919	0.918	0.737
^{122}Sn	1.141	1.142	0.872
^{122}Te	0.564	0.564	0.731
^{124}Te	0.603	0.602	0.725
^{126}Te	0.666	0.667	0.727
^{126}Xe	0.389	0.389	0.665
^{132}Ba	0.465	0.464	0.658

3.4 pnQRPA Calculations

In this step we constructed the 2_1^- state of the odd-odd nuclei by using the pnQRPA. In the pnQRPA matrix the particle-particle part was scaled by the particle-particle interaction parameter g_{pp}. We adjusted g_{pp} to reproduce roughly the experimental energy gap values between the 2_1^- state and the 1_1^+ state. We present these gaps as functions of g_{pp} in Figs 11-13. For example, we present in Fig. 13 the energies of the 2_1^- and 1_1^+ states of ^{132}La as functions of g_{pp}. The experimental gap between 2_1^- and 1_1^+ states is 182.62 keV which correspond to g_{pp}=1.272.

In some cases we could not determine the g_{pp} values and one of them is ^{74}As. The computed 1_1^+ state is lower than 2_1^- state for any g_{pp} values in the range 0.2-1.3, opposite to the experimental situation, see Fig 11. For some nuclei like ^{82}Br, it was impossible to find a suitable g_{pp} value even if the 2_1^- state was lower than 1_1^+ state like in experiment because the energy gap was extremely large compared with the experimental energy gap, see Fig 12. Another reason is that there is no experimental data, like for ^{124}I. For these nuclei we study, as you will see in section 3.5, how much g_{pp} affects the log (ft) values and which g_{pp} values are suitable for each. Tables 4 and 5 show the adopted g_{pp} values.

Table 4: The values of g_{pp} parameter for nuclei decaying via β^+.

Nucleus	Difference between energy levels 1_1^+ and 2_1^- Experimental (keV)	Theoretical (keV)	g_{pp}
^{72}As	46.025	46.025	0.862
^{74}As	206.559	206.15	1.351
^{76}As	44.425	1756.4	0.9
^{84}Rb	1007.6	1007.27	1.3483
^{86}Rb	488.24	488.37	1.439
^{122}Sb	121.497	594.99	0.9
^{124}I	-	606.67	0.9
^{126}I	56.43	669.63	0.9
^{132}Ba	182.073	182.62	1.272

3.5 Beta Calculation

In this step we show results of the beta calculations. We also studied how our calculated results depend on g_{pp} and the value of the axial vector coupling constant g_A, this is done in Tables 6-8 for the transition form 2_{gs}^- to 0_{gs}^+ (other

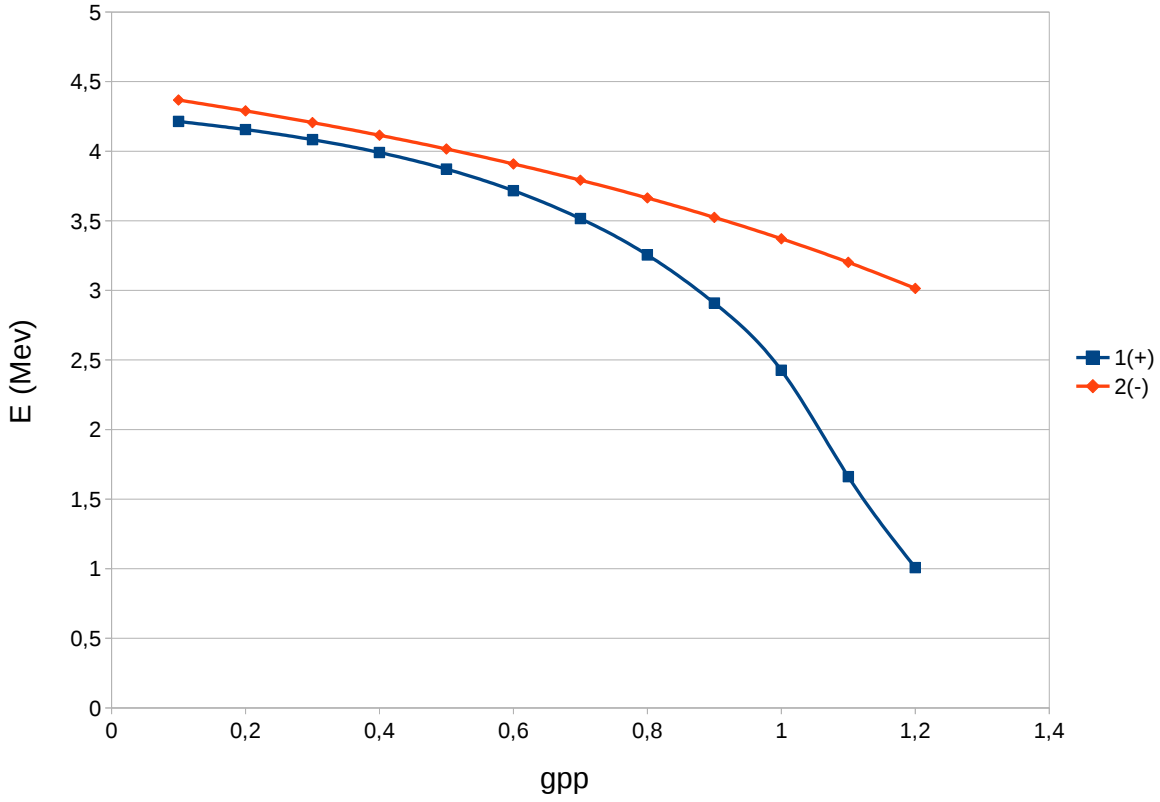

Figure 11: The energies of the 1_1^+ and 2_1^- states for ^{74}As relative to the ground state of ^{74}Se as functions of the g_{pp} parameter. This scheme shows how some times it is impossible to determine the g_{pp} value because the energy level 1_1^+ is lower than 2_1^-, opposite to the experimental result.

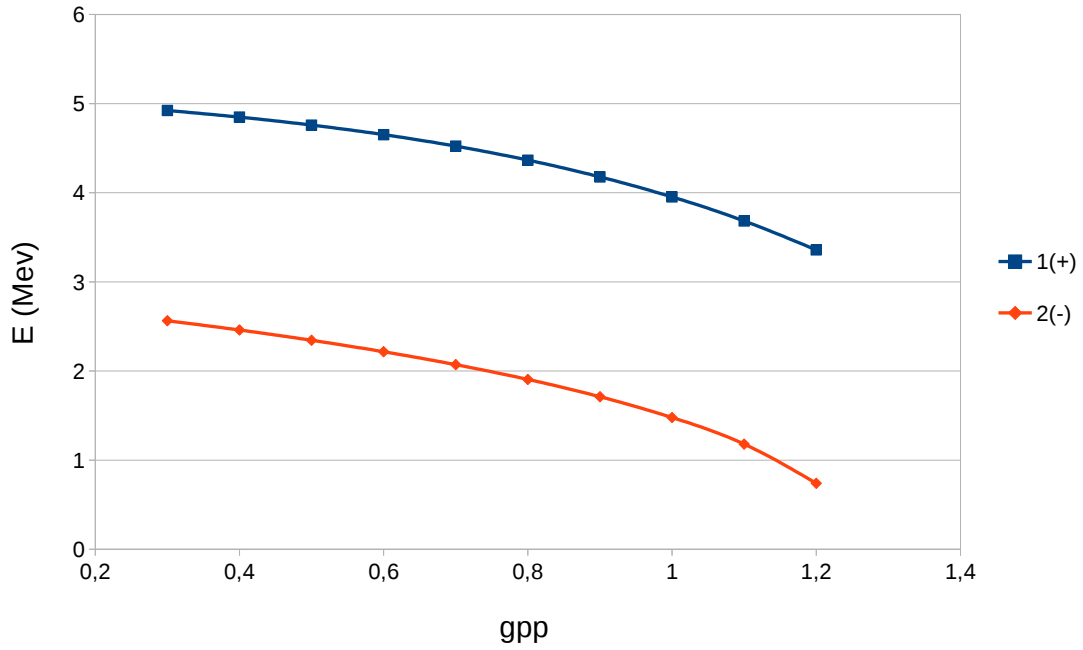

Figure 12: The energies of the 1_1^+ and 2_1^- states for ^{82}Br relative to the ground state of ^{82}Kr as functions of the g_{pp} parameter. This scheme shows how some times it is impossible to determine the g_{pp} value because the energy level 1_1^+ is higher than 2_1^- in the calculations.

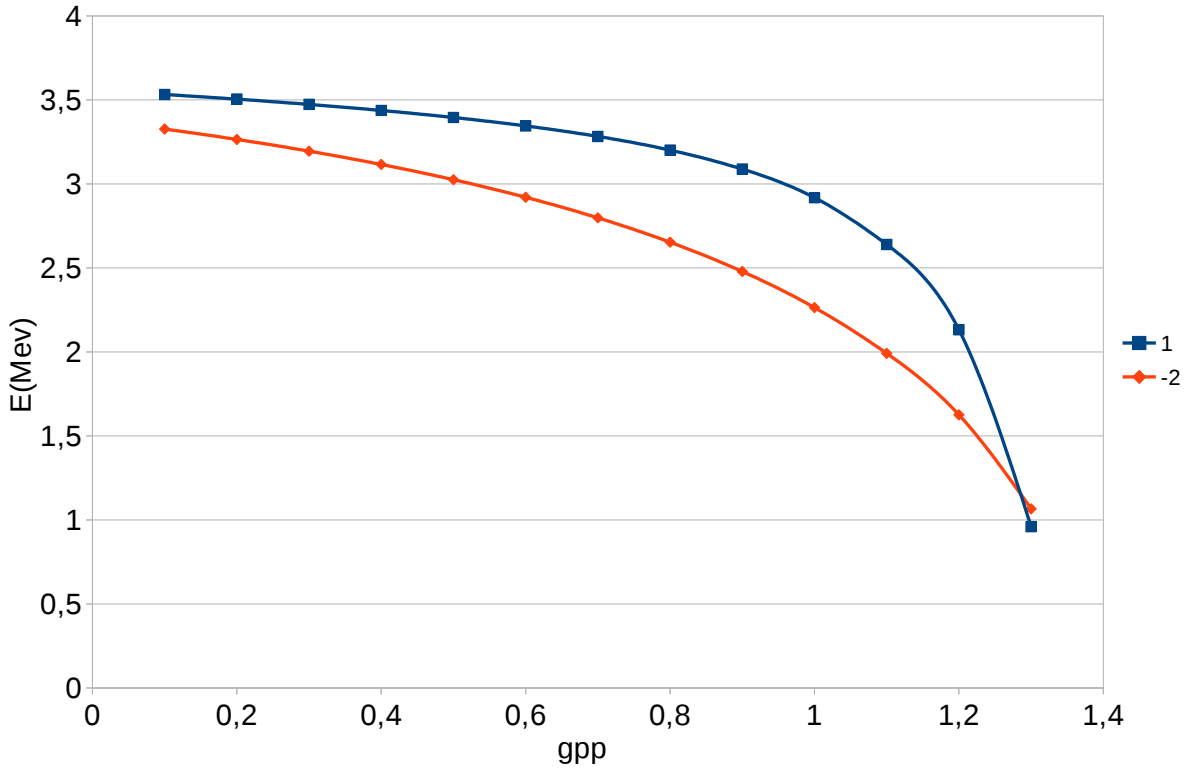

Figure 13: The energies of the 1_1^+ and 2_1^- states for ^{132}La relative to the ground state of ^{132}Ba as functions of the g_{pp} parameter. This scheme shows how some times it is possible to determine by this procedure the g_{pp} value.

Table 5: The values of g_{pp} parameter for nuclei decaying via β^-.

Nucleus	Difference between energy levels 1_1^+ and 2_1^- Experimental (keV)	Theoretical (keV)	g_{pp}
^{74}As	173.136	-615.67	0.9
^{76}As	44.425	44.04	1.1605
^{78}As	277.33	277.77	1.3481
^{82}Br	29.113	1583.67	0.9
^{84}Br	408.24	2025.38	0.9
^{84}Rb	1007.6	1006.5	0.66
^{86}Rb	488.24	488.29	1.1588
^{88}Rb	2391.7	1492.22	0.9
^{92}Y	1384.914	1443.6	0.9
^{94}Y	1427.717	40.31	0.9
^{122}Sb	121.149	121.15	1.119
^{122}I	56.43	58.62	1.169

transitions have a similar behaviour). Fig 14 shows the relation between $\log(ft)$ and g_{pp} values . It is clear that $\log(ft)$ is only weekly dependent on g_{pp} values.

We present in Tables 9 - 12 the computed $\log(ft)$ values. In these tables we notice a difference between experimental and theoretical values. This difference can be explained by the fact that nuclear matrix elements predicted by pnQRPA are much larger than the observed ones [6].

Table 6: The $\log(ft)$ values for β^- transition ^{94}Y$\longrightarrow$ ^{94} Zr for g_{pp}=0.7 and different g_A values.

g_{pp}=0.7 and g_A=0.75	$\log(ft)$	
Transition ^{94}Y$\longrightarrow$ ^{94}Zr	Theoretical	Experimental
$(2_1^-) \longrightarrow (0_{gs}^-)$	9.506	9.35

g_{pp}=0.7 and g_A=1.00	$\log(ft)$	
Transition ^{94}Y$\longrightarrow$ ^{94}Zr	Theoretical	Experimental
$(2_1^-) \longrightarrow (0_{gs}^-)$	9.2562	9.35

g_{pp}=0.7 and g_A=1.25	$\log(ft)$	
Transition ^{94}Y$\longrightarrow$ ^{94}Zr	Theoretical	Experimental
$(2_1^-) \longrightarrow (0_{gs}^-)$	9.0623	9.35

Table 7: The log(ft) values for β^- transition ^{94}Y$\longrightarrow$ ^{94}Zr for g$_{\rm pp}$=0.8 and different g$_{\rm A}$ values.

g$_{\rm pp}$=0.8 and g$_{\rm A}$=0.75	log(ft)	
Transition ^{94}Y$\longrightarrow$ ^{94}Zr	Theoretical	Experimental
$(2_1^-) \longrightarrow (0_{gs}^-)$	9.4936	9.35

g$_{\rm pp}$=0.8 and g$_{\rm A}$=1.00	log(ft)	
Transition ^{94}Y$\longrightarrow$ ^{94}Zr	Theoretical	Experimental
$(2_1^-) \longrightarrow (0_{gs}^-)$	9.2438	9.35

g$_{\rm pp}$=0.8 and g$_{\rm A}$=1.25	log(ft)	
Transition ^{94}Y$\longrightarrow$ ^{94}Zr	Theoretical	Experimental
$(2^-) \longrightarrow (0_{gs}^-)$	9.05	9.35

Table 8: The log (ft) values for β^- transition ^{94}Y$\longrightarrow$ ^{94}Zr for g$_{\rm pp}$=0.9 and different g$_{\rm A}$ values.

g$_{\rm pp}$=0.9 and g$_{\rm A}$=0.75	log(ft)	
Transition ^{94}Y$\longrightarrow$ ^{94}Zr	Theoretical	Experimental
$(2_1^-) \longrightarrow (0_{gs}^-)$	9.4877	9.35

g$_{\rm pp}$=0.9 and g$_{\rm A}$=1.00	log(ft)	
Transition ^{94}Y$\longrightarrow$ ^{94}Zr	Theoretical	Experimental
$(2_1^-) \longrightarrow (0_{gs}^-)$	9.2379	9.35

g$_{\rm pp}$=0.9 and g$_{\rm A}$=1.25	log(ft)	
Transition ^{94}Y$\longrightarrow$ ^{94}Zr	Theoretical	Experimental
$(2_1^-) \longrightarrow (0_{gs}^-)$	9.044	9.35

The results are depicted in Figures 15a -18b to make the picture clearer. Let us take first a look at the Figures 15a-15c where both the experimental and theoretical log(ft) values for first forbidden unique beta-decay transitions are depicted (when both are available). The computed log(ft) values for the unique β^- transition to the states 0_{gs}^+ and, 0_1^+ have a general tendency. In this tendency the theoretical values are smaller than the experimental ones. Only in two cases, ^{82}Br and ^{88}Rb, the theoretical log(ft) are slightly larger than the experimental ones. This general tendency can be explained by the fact that the nuclear matrix elements predicted by pnQRPA are much larger than

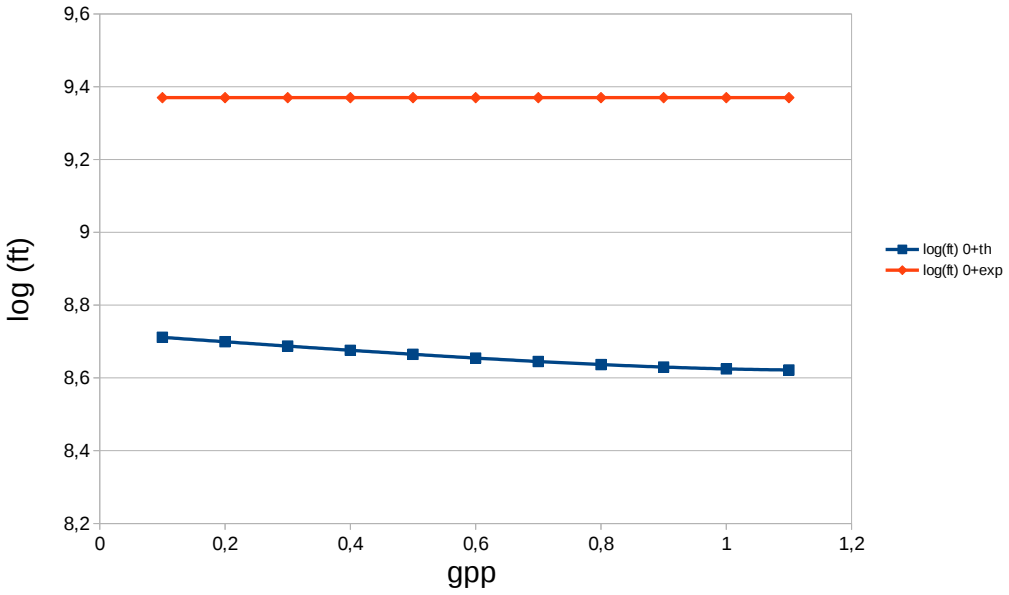

Figure 14: The relation between $\log(ft)$ and g_{pp} for the decay of ^{74}As to ^{74}Se.

Table 9: The $\log(ft)$ values for the nuclei decaying via unique β^-.

$g_A = 1.00$		$\log(ft)$ $(2_1^-$ to $0_{gs}^+)$		$\log(ft)$ $(2_1^-$ to $0_1^+)$		$\log(ft)$ $(2_1^-$ to $4_1^+)$	
Nucleus	g_{pp}	Theoretical	Experimental	Theoretical	Experimental	Theoretical	Experimental
^{74}As	0.9	8.6337	9.37^{1u}	11.01	-	12.65	-
^{76}As	1.1605	8.7818	9.73^{1u}	10.33	10.29^{1u}	12.03	11.16^{1u}
^{78}As	1.3481	9.1568	9.64^{1u}	10.08	10.51^{1u}	11.83	10.26^{1u}
^{82}Br	0.9	8.9836	8.88^{1u}	10.47	10.40^{1u}	12.20	10.5^{1u}
^{84}Br	0.9	8.9599	9.46^{1u}	10.23	10.8^{1u}	11.90	$>9.8^{1u}$
^{84}Rb	0.66	8.8615	9.4^{1u}	-	-	-	-
^{86}Rb	1.1838	9.1259	9.4399^{1u}	-	-	-	-
^{88}Rb	0.9	9.1206	9.2455^{1u}	11.05	-	13.85	-
^{92}Y	0.9	9.0281	9.27^{1u}	12.12	9.58^{1u}	12.83	9.75^{1u}
^{94}Y	0.9	9.2379	9.35^{1u}	11.39	9.87^{1u}	12.13	9.39^{1u}
^{122}Sb	1.119	9.4999	9.654^{1u}	10.36	10.32^{1u}	11.93	10.83^{1u}
^{126}I	1.169	9.4952	9.649^{1u}	9.91	-	11.50	-

Table 10: The log(ft) values for the nuclei decaying via non unique β^-.

$g_A = 1.00$		log(ft) (2_1^- to 2_1^+)		log(ft) (2_1^- to 2_2^+)	
Nucleus	g_{pp}	Theoretical	Experimental	Theoretical	Experimental
^{74}As	0.9	9.39	7.63	10.61	>7.1
^{76}As	1.1605	8.19	8.12	8.70	8.21
^{78}As	1.3481	7.15	7.91	8.13	7.61
^{82}Br	0.9	7.48	7.91	9.08	7.93
^{84}Br	0.9	6.58	7.70	7.10	7.21
^{84}Rb	0.66	7.37	-	-	-
^{86}Rb	1.1838	6.97	7.932	-	-
^{88}Rb	0.9	7.84	7.768	9.34	7.512
^{92}Y	0.9	7.46	8.56	8.34	8.73
^{94}Y	0.9	6.61	7.181	7.76	7.87
^{122}Sb	1.119	8.51	7.614	7.55	7.70
^{126}I	1.169	7.52	7.833	7.25	7.551

Table 11: The log(ft) values for the nuclei decaying via unique β^+.

$g_A = 1.00$		log(ft) (2_1^- to 0_{gs}^+)		log(ft) (2_1^- to 0_1^+)		log(ft) (2_1^- to 4_1^+)	
Nucleus	g_{pp}	Theoretical	Experimental	Theoretical	Experimental	Theoretical	Experimental
^{72}As	0.862	9.4123	9.84^{1u}	10.57	10.56^{1u}	12	10.34^{1u}
^{74}As	1.3518	8.9731	9.7^{1u}	10.09	10.34^{1u}	11.51	11.28^{1u}
^{76}As	0.9	8.7390	-	-	-	-	-
^{84}Rb	1.3483	9.1526	9.509^{1u}	6.39	-	6.39	-
^{86}Rb	1.4390	9.0703	9.78^{1u}	-	-	-	-
^{122}Sb	0.9	8.4017	8.99^{1u}	-	-	-	-
^{124}I	0.9	8.5020	9.27^{1u}	10.69	10.30^{1u}	12.05	11.17^{1u}
^{126}I	0.9	8.3852	9.201^{1u}	6.6 0	10.15^{1u}	6.60	$\geq 12.4^{1u}$
^{132}Ba	1.272	8.4538	9.48^{1u}	10.34	10.0^{1u}	11.89	9.6^{1u}

Table 12: The log(ft) values for the nuclei decaying via non unique β^+.

$g_A = 1.00$		log(ft) (2_1^- to 2_1^+)		log(ft) (2_1^- to 2_2^+)	
Nucleus	g_{pp}	Theoretical	Experimental	Theoretical	Experimental
^{72}As	0.862	7.51	7.208	8.10	7.692
^{74}As	1.351	6.9	6.96	7.23	8.247
^{76}As	0.9	-	-	-	-
^{84}Rb	1.3483	6.80	7.114	6.38	8.085
^{86}Rb	1.439	-	-	-	-
^{124}I	0.9	6.81	7.49	7.58	7.87
^{126}I	0.9	7.13	7.452	6.59	7.629
^{132}Ba	1.272	6.35	7.5	7.42	7.2

the observed ones [6]. In contrast if one takes a look at the computed values of the transitions to the 4_1^+ state, the previous general tendency becomes reversed: the theoretical values became bigger than the experimental ones. Only in one case ,^{124}I, the theoretical $\log(ft)$ is larger than the experimental one. This general tendency can be explained by the fact that the nuclear matrix elements predicted by pnQRPA are smaller than the observed ones [6].

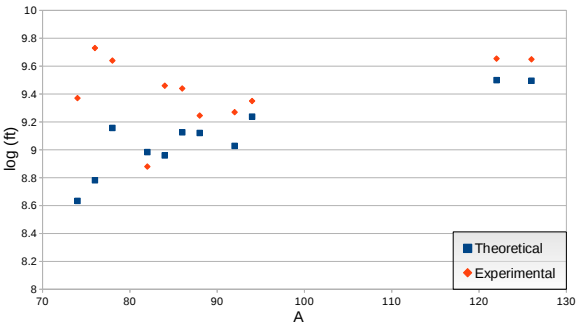

(a) Transition from 2_1^- to 0_{gs}^+

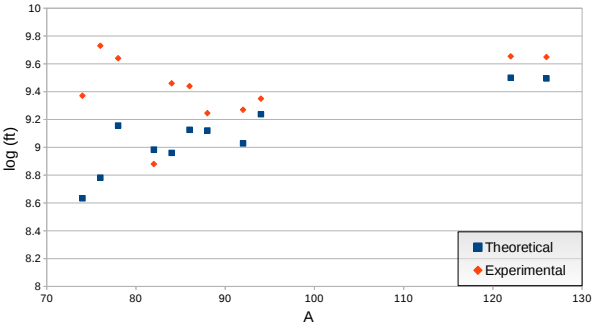

(b) Transition from 2_1^- to 0_1^+

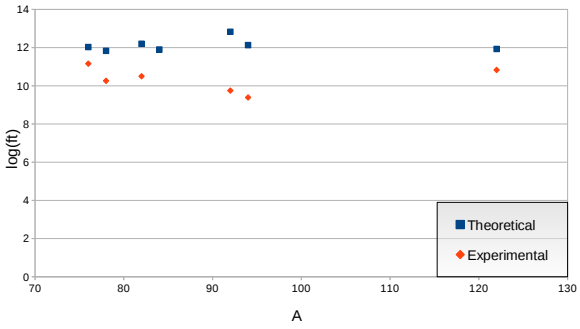

(c) Transition from 2_1^- to 4_1^+

Figure 15: Experimental and theoretical $log(ft)$ values for the unique β^- transitions.

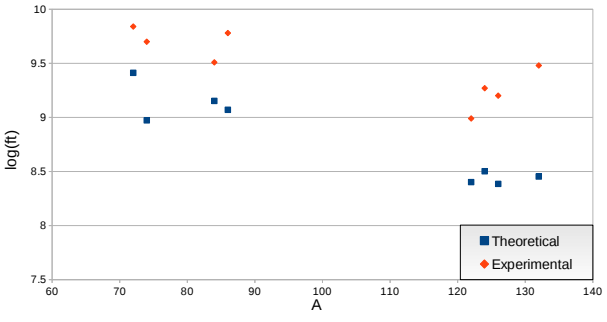

(a) Transition from 2_1^- to 0_{gs}^+

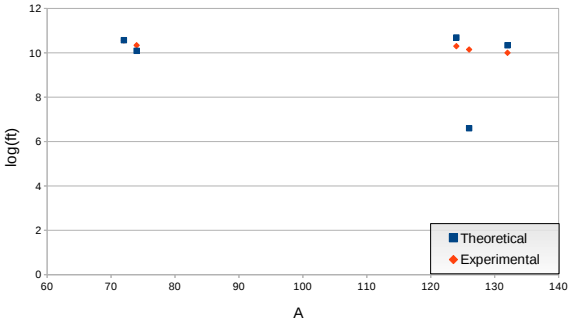

(b) Transition from 2_1^- to 0_1^+

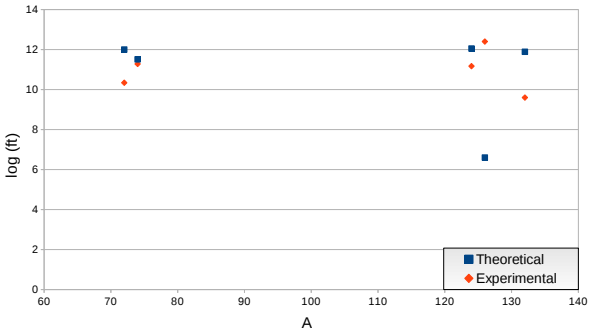

(c) Transition from 2_1^- to 4_1^+

Figure 16: Experimental and theoretical $log(ft)$ values for the unique β^+ transitions.

Second feature one can notice by looking at the Figures 15a-15b, for the β^- transitions to the 0^+ ground states and 0_1^+, is that the differences between theoretical and experimental values become smaller by increasing the mass number. This features is not present for the transition to the 4_1^+ state.

By looking at the Figs 16a-16c the obtained results for unique β^+ transition. One can notice clear feature for the computed $\log(ft)$ values for the transitions to the 0_{gs}^+. These theoretical values are always smaller than the experimental ones. This feature can be explained by fact that the nuclear matrix elements predicted by pnQRPA are much larger than the experimental ones. For the transitions to the 0_1^+ and 4_1^+ one can not notice any clear feature. In general one can mention that the theoretical and the experimental results are much closer comparing with the analogous unique β^- transition.

In the Figures 17a-18b both the experimental and theoretical $\log(ft)$ values for first forbidden non-unique beta decays transitions are depicted (when both are available). One can notice that the differences between theoretical and experimental values have less fluctuations. In the other words the differences between theoretical and experimental values are closer to the average of differences. Also one can mention that the results for larger masses are somewhat better.

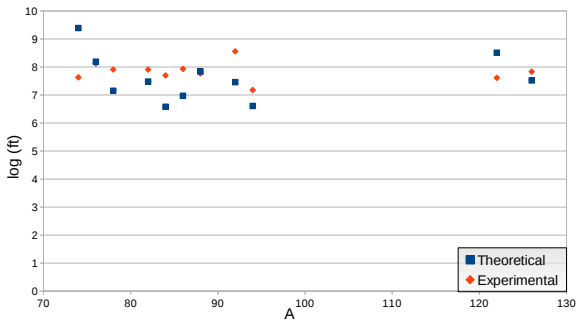

(a) Transition from 2_1^- to 2_1^+

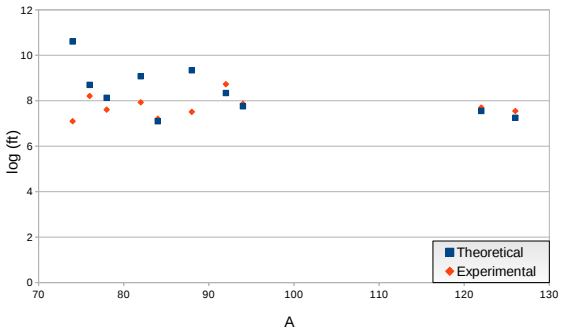

(b) Transition from 2_1^- to 2_2^+

Figure 17: Experimental and theoretical $log(ft)$ values for the non-unique β^- transitions.

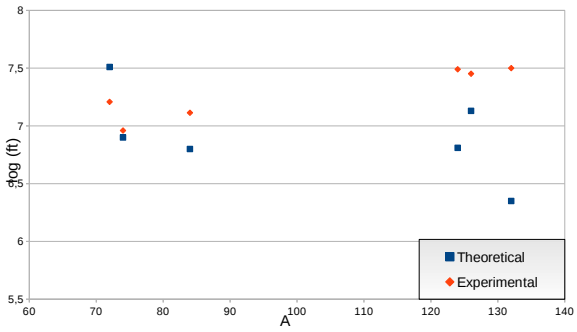

(a) Transition from 2_1^- to 2_1^+

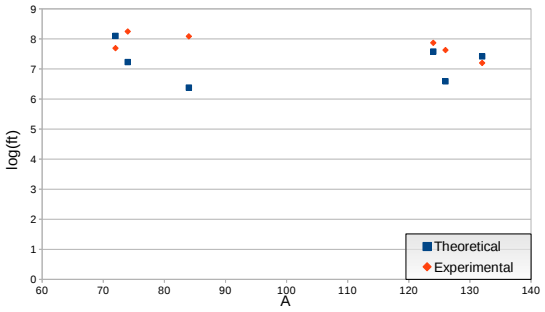

(b) Transition from 2_1^- to 2_2^+

Figure 18: Experimental and theoretical $log(ft)$ values for the non-unique β^+ transitions.

4 Conclusion

In this thesis the first-forbidden (both unique and non-unique) beta decays were studied. The ground state of the even-even nucleus is obtained from the BCS theory [1, 2], where the interaction was scaled by a constant $g_{\mathrm{p}}^{\mathrm{pair}}$ for protons and $g_{\mathrm{n}}^{\mathrm{pair}}$ for neutrons. The quasiparticle random-phase approximation (QRPA) was adopted to construct the excited states of the even-even nuclei. There the QRPA matrix was scaled by parameter called g_{ph}. The proton-neutron quasiparticle random-phase approximation (pnQRPA) was also adopted to construct the excited states of the odd-odd nucleus. The particle-particle part of the pnQRPA matrix was scaled by the particle-particle interaction parameter $\mathrm{g_{pp}}$. The results of this work are comparative β decay half-lives, $\log(ft)$, for the transitions from the 2^- ground states of the odd-odd nuclei to the 0^+ ground states, 0_1^+, 4_1^+, 2_1^+ and 2_2^+ states of the even-even nuclei. These theoretical estimates are given in Tables 9-12.

Finally the obtained results are compared with experimental data, when they are available and depicted in Figures 15a -18b. Two features had been noticed for the first forbidden unique β^- transition. First one, the computed $\log(ft)$ values for transition to the states 0^+ ground states and 0_1^+ have general tendency. It was found that the theoretical values are smaller than the experimental ones. This tendency is explained by the fact that the nuclear matrix elements predicted by pnQRPA are much larger than the observed ones [6]. This previous feature was noticed also for the transitions to 4_1^+

states but it was inverse. The computed $\log(ft)$ values for transition to the 0^+ ground states and 0_1^+ showed that the differences between theoretical and experimental values become smaller by increasing the mass number. Where as these features are not clear for the transition to the 4_1^+ state. For the first forbidden unique β^+ transitions there are also two features had been noticed. First feature the computed $\log(ft)$ values for the transitions to the 0_{gs}^+ were always smaller than the experimental ones.This feature is explained by the fact that the nuclear matrix elements predicted by pnQRPA are much larger than the observed ones. Second feature noticed that the theoretical and the experimental results are much closer comparing with the analogous unique β^- transitions. For first-forbidden non-unique beta decays transitions the obtained results had less deviation from data than the results of the first-forbidden unique beta decays transitions.

In the end, one can mention that the obtained results for the transition 2_{gs}^- to 0_{gs}^+ are used in analysing the suppression of spin-dipole (SD) nuclear matrix elements (NMEs) for these β decays, and this was done in article [6]. These NMEs are associated with the $J^\pi = 2^-$ component of $0\nu\beta\beta$ matrix element and the cross sections of the medium-energy neutrino-nuclear interactions. Now the $0\nu\beta\beta$ decays of several isotopes are under extensive experimental and theoretical study to access the Majorana properties of neutrinos and their absolute mass scale [7, 8, 9, 10]. Then a reliable value of $0\nu\beta\beta$ NME is required to design an optimum $0\nu\beta\beta$ detector and to deduce the neutrino mass from the measured $0\nu\beta\beta$ decay rate in case it is observed.

References

[1] Jouni Suhonen, *From Nucleons to Nucleus: Concept of Microscopic Nuclear Theory* (Springer, Berlin, 2007)

[2] J. Toivanen , J. Suhonen, Phys. Rev. C 57 (1998) 1237

[3] National Nuclear Data Center, http//www.nndc.bnl.gov

[4] N. B. Gove, M. J. Martin, Nucl. Data Tables 10, 205 (1971).

[5] H.Behrens, W.Buhring: *Electron Radial Wave Functions and Nuclear Beta Decay* (Clarendon, Oxford, 1982)

[6] H. Ejiri, N. Soukouti, J. Suhonen, Phys. Lett. B 729 (2014) 27.

[7] J. Vergados, H. Ejiri, F. Simkovic, Rep. Prog. Phys. 75 (2012) 106301.

[8] S. R. Elliott and P. Vogel, Ann. Rev. Nucl. Part. Sci. 52 (2002) 115.

[9] H. Ejiri, J. Phys. Soc. Jpn. 74 (2005) 2101.

[10] F. Avignone, S. Elliott, J. Engel, Rev. Mod. Phys. 80 (2008) 481.